Casimir repulsive-attractive transition between liquid-separated dielectric metamaterial and metal

Yingqi Ye, Qian Hu, Qian Zhao,* and Yonggang Meng
State Key Laboratory of Tribology, Department of Mechanical Engineering, Tsinghua University, Beijing 100084, China

(Received 24 April 2018; revised manuscript received 19 June 2018; published 6 July 2018)

Herein, the repulsive-attractive transition, regarded as a stable equilibrium, between gold and dielectric metamaterials (based on Mie resonance) immersed in various fluids was studied. This transition is owing to the interplay of the gravitational, buoyant, and Casimir forces among different geometries containing parallel plates and spheres levitated over substrates. It was found that Mie metamaterials allowed a wider range of separation distance for stable equilibrium than was possible with natural materials. The relationship between the separation distance for stable equilibrium and the constructive parameters of the Mie metamaterial and the geometric parameters of the system was investigated, and simple rules for tuning the equilibrium position by modifying the constructive parameters of the Mie metamaterial was provided. These results are promising for potential applications in frictionless suspension in micro/nanofabrication technologies.

DOI: 10.1103/PhysRevB.98.035410

I. INTRODUCTION

The Casimir effect, which exists between neutral bodies at zero temperature owing to vacuum fluctuations, was first predicted by Casimir in 1948 [1]. Following this work, Lifshitz extended the theory from two semi-infinite perfectly electric conductor slabs to realistic dielectrics [2]. Owing to the irreversible adhesion of neighboring elements in micro/nanoelectromechanical devices caused by the Casimir attraction, methods to alter the attraction to repulsion becomes important. One practical way to gain Casimir repulsion is to immerse two interacting objects in a fluid and thereby satisfy $\varepsilon_1(i\xi) < \varepsilon_{\text{fluid}}(i\xi) < \varepsilon_2(i\xi)$ over a broad range of imaginary frequencies ξ, where $\varepsilon_{\text{fluid}}(i\xi)$, $\varepsilon_1(i\xi)$, and $\varepsilon_2(i\xi)$ are the dielectric permittivities of the fluid and the two interacting bodies, respectively [3]. Remarkable progress has been made with theoretical calculations and experimental measurements to identify various liquids that obtain a repulsive force [4–7]. It has been demonstrated in several works that a proper combination of two materials and liquid can give rise to a repulsive-attractive transition, which occurs when the electromagnetic characteristics of one of the interacting objects are close to that of the fluid over some frequency range [8,9]. This unique behavior is desirable for potential applications in frictionless suspension and micro/nanofabrication technology. However, the behavior occurs only in a few combinations of natural materials and the transition takes place in a limited range of separation distance owing to the limited material choices.

On the other hand, the Casimir force can become repulsive if, of the two interacting objects, one is primarily electric while the other is primarily magnetic based on Boyer's theory [10]. In this way, the most challenging problem is to select or construct a material with sufficiently strong magnetic response and relatively low dielectric permittivity, which is almost impossible for natural magnetic materials. Numerous different artificial materials have been studied, including chiral metamaterials [11–13], hyperbolic metamaterials [14], electromagnetic metamaterials based on LC-circuit resonance [15,16] or Mie resonance [17], and several other materials [18–24]. These studies have provided many methods to minimize attraction but only a few theoretical predictions of the repulsion.

Here, we propose an approach to give rise to the repulsive-attractive transition using the combination of a dielectric metamaterial and a metal immersed in a fluid. We chose the former because the metamaterial, with its designable electric and magnetic properties, is expected to be more suitable to meet the requirements necessary for transition to occur. The metamaterial used herein was based on Mie resonance and was constructed by dielectric spherical particles dispersed in a host medium. This metamaterial was chosen in this study to display repulsive-attractive transitions because of its relatively low dielectric permittivity and high magnetic permeability [25–28]. Furthermore, it can be treated as an isotropic material when the spherical particles are identical and dispersed homogeneously [29]. The dielectric permittivity and magnetic permeability of the nanoparticle-based metamaterial depend on the constructive parameters, which mainly include the filling factor of the particles in the unit cell and the particle size and material.

Schematics of the plate-plate and sphere-plate geometries in both vertical and horizontal arrangements are illustrated in Fig. 1. In the horizontal setup, levitation occurs with the balance of gravitational, buoyant, and Casimir forces, while only Casimir force needs to be considered in the vertical arrangement. In this paper, we theoretically analyzed the deviation of the transition position between the Mie metamaterial slab and the gold slab/sphere immersed in various liquids as a function of multiple parameters, including the Mie metamaterial constructive parameters and geometric parameters of the system. Using this theoretical study, we established a rule to guide the design of Mie metamaterials to obtain a specific separation distance of equilibrium.

*zhaoqian@mail.tsinghua.edu.cn

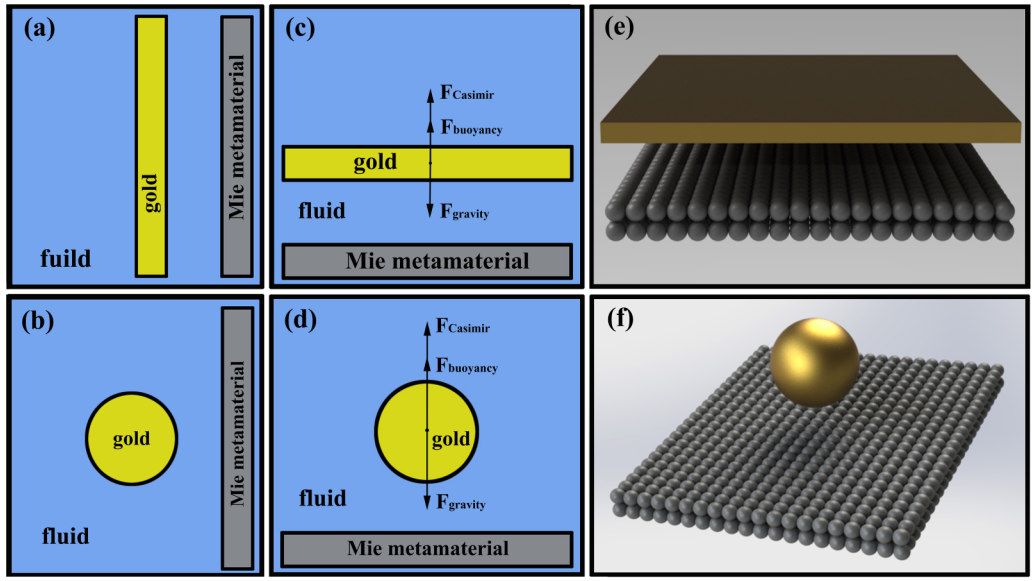

FIG. 1. Schematic images of liquid-separated gold and Mie metamaterial systems with various geometries: (a) parallel plate-plate and (b) sphere-plate systems in a vertical arrangement, (c) parallel plate-plate and (d) sphere-plate systems in a horizontal arrangement. Schematic images of (e) gold film or (f) gold sphere suspended over a Mie metamaterial substrate.

II. MODEL AND THEORETICAL FRAMEWORK

The Casimir force per unit area between two parallel plates immersed in a fluid separated by a distance d at zero temperature can be expressed as

$$F_C = \frac{\hbar}{\pi}\int_0^\infty d\xi \iint \frac{d^2\mathbf{k}_\parallel}{(2\pi)^2} K_{\text{fluid}} \times \sum_{p=\text{TE,TM}} \frac{r_1^p(i\xi,k) r_2^p(i\xi,k) e^{-2K_{\text{fluid}}d}}{1 - r_1^p(i\xi,k) r_2^p(i\xi,k) e^{-2K_{\text{fluid}}d}}, \quad (1)$$

where the integral is carried out over the imaginary frequency ξ instead of the real frequency ω to avoid singularities, $\hbar$ is the reduced Planck constant, $\mathbf{k}_\parallel$ is the wave vector parallel to the surface, and $K_{\text{fluid}} = \sqrt{\varepsilon_{\text{fluid}}(i\xi)\xi^2/c^2 + k^2}$, where c is the speed of light; $r^p_{1(2)}$ are diagonal elements of the reflection matrices for the two interacting objects, where off-diagonal elements are zero in our setup without entanglement of the transverse electric (TE) and transverse magnetic (TM) modes. Further, $r^p_{1(2)}$ can be written as

$$r^{\text{TE}}_{1(2)} = \frac{\mu_{1(2)}(i\xi)K_{\text{fluid}} - \sqrt{k_{||}^2 + \varepsilon_{1(2)}(i\xi)\mu_{1(2)}(i\xi)\xi^2/c^2}}{\mu_{1(2)}(i\xi)K_{\text{fluid}} + \sqrt{k_{||}^2 + \varepsilon_{1(2)}(i\xi)\mu_{1(2)}(i\xi)\xi^2/c^2}}, \quad (2)$$

$$r^{\text{TM}}_{1(2)} = \frac{\varepsilon_{1(2)}(i\xi)K_{\text{fluid}} - \sqrt{k_{||}^2 + \varepsilon_{1(2)}(i\xi)\mu_{1(2)}(i\xi)\xi^2/c^2}}{\varepsilon_{1(2)}(i\xi)K_{\text{fluid}} + \sqrt{k_{||}^2 + \varepsilon_{1(2)}(i\xi)\mu_{1(2)}(i\xi)\xi^2/c^2}}, \quad (3)$$

where $\varepsilon_{1(2)}(i\xi)$ and $\mu_{1(2)}(i\xi)$ are the dielectric permittivities and magnetic permeabilities of the two interacting bodies, respectively. The Casimir force between a sphere of radius R_s and a plate can be described by the proximity-force approximation (PFA), which is widely used in calculations of curved objects [30–32]. Here, the PFA relation can be written as $F_{\text{PFA}} = 2\pi R_s E$, where E is the interaction energy per unit area in a parallel-plate system composed of the same materials and at the same separation distance as in a sphere-plate system. The effect of a finite plate thickness on the Casimir force is also considered by replacing the reflection coefficients with generalized Fresnel coefficients [33,34].

We construct the Mie metamaterial by homogeneously dispersing dielectric spherical particles in air. Based on the extended Maxwell-Garnett theory [29], the dielectric permittivity ε_{Mie} and magnetic permeability μ_{Mie} of the Mie metamaterial comprising particles of radius R_p and a filling factor f at a real frequency can be expressed as

$$\varepsilon_{\text{Mie}} = \frac{x^3 - 3if T_1^{\text{E}}}{x^3 + \frac{3}{2}if T_1^{\text{E}}}, \quad (4)$$

$$\mu_{\text{Mie}} = \frac{x^3 - 3if T_1^{\text{H}}}{x^3 + \frac{3}{2}if T_1^{\text{H}}}, \quad (5)$$

where $x = \omega R_p/c$, and T_1^{E} and T_1^{H} are the electric-dipole and magnetic-dipole coefficients of the scattering matrix of a single particle, and can be given by the following formula:

$$T_1^{\text{E}} = \frac{j_1(x_p)[x j_1(x)]'\varepsilon_p(\omega) - j_1(x)[x_p j_1(x_p)]'}{h_1^+(x)[x_p j_1(x_p)]' - j_1(x_p)[x h_1^+(x)]'\varepsilon_p(\omega)}, \quad (6)$$

$$T_1^{\text{H}} = \frac{j_1(x_p)[x j_1(x)]'\mu_p(\omega) - j_1(x)[x_p j_1(x_p)]'}{h_1^+(x)[x_p j_1(x_p)]' - j_1(x_p)[x h_1^+(x)]'\mu_p(\omega)}, \quad (7)$$

where $x_p = \sqrt{\varepsilon_p(\omega)\mu_p(\omega)}R_p/c$, where $\varepsilon_p(\omega)$ and $\mu_p(\omega)$ are the permittivity and permeability of the particle material, respectively; j_1 is the first-order spherical Bessel function; h_1^+ is the first-order Hankel function; and $[z j_1(z)]' = d[z j_1(z)]/dz|_{z=x}$, etc. To apply the permittivity and permeability of the Mie metamaterial in the Casimir force calculation formula, $\varepsilon_{\text{Mie}}(\omega)$ and $\mu_{\text{Mie}}(\omega)$ are converted to the imaginary

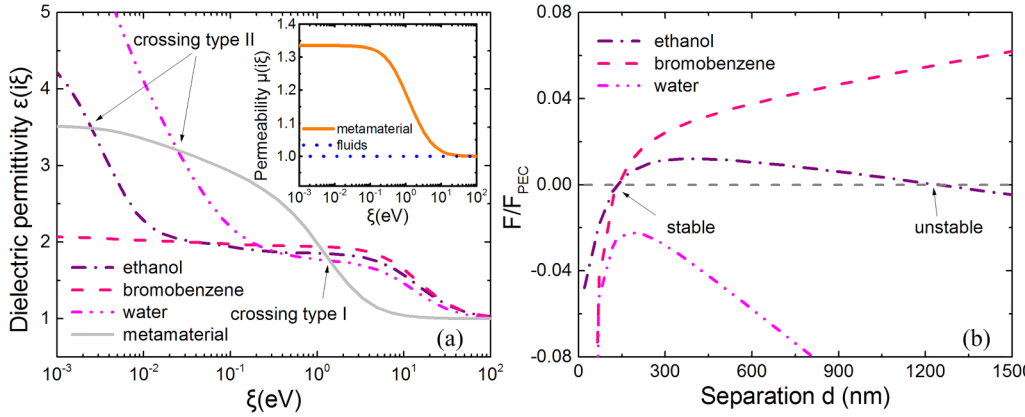

FIG. 2. (a) Dielectric permittivity of ethanol, bromobenzene, pure water, and Mie metamaterial comprising silicon particles ($R_p = 100$ nm, $f = 0.5$) as a function of imaginary frequency. (b) Casimir force (F) between gold and Mie metamaterial semi-infinite plates immersed in ethanol, bromobenzene, and pure water. The F values are normalized by the Casimir force between perfect electric conductors in vacuum (F_{PEC}).

frequency domain according to the Kramers-Kronig relation [2]:

$$\varepsilon(i\xi) = 1 + \frac{2}{\pi}\int_0^\infty \frac{\omega\varepsilon''(\omega)}{\xi^2+\omega^2}d\omega, \tag{8}$$

$$\mu(i\xi) = 1 + \frac{2}{\pi}\int_0^\infty \frac{\omega\mu''(\omega)}{\xi^2+\omega^2}d\omega, \tag{9}$$

where $\varepsilon''(\omega)$ and $\mu''(\omega)$ are, respectively, the imaginary parts of the permittivity and permeability of the material calculated at a real frequency.

III. RESULTS AND DISCUSSION

We investigated the combination of fluid and Mie metamaterial whereby the transition from repulsion to attraction of the Casimir force will occur first. Herein, the parallel-plate system in a vertical arrangement is considered, where gravitational and buoyant forces are not taken into account. As mentioned above, a repulsive Casimir force can be gained in the conditions when $\varepsilon_1(i\xi) < \varepsilon_{fluid}(i\xi) < \varepsilon_2(i\xi)$ is satisfied or an object that is primarily electric interacts with another object that is primarily magnetic. In our system, gold and the Mie metamaterial were selected as the two interacting bodies. With this system, $\varepsilon_{fluid}(i\xi) < \varepsilon_{gold}(i\xi)$ is assumed to be satisfied over almost the entire range of frequencies because $\varepsilon_{gold}(i\xi)$ is rather large. Therefore, the remaining requirement $\varepsilon_{Mie}(i\xi) < \varepsilon_{fluid}(i\xi)$ needs to be examined. Gold and all of the selected liquids (i.e., ethanol, bromobenzene, and pure water) herein were nonmagnetic with $\mu = 1$, while the permeability of the Mie metamaterial depends on its constructive parameters. The dielectric permittivity as a function of imaginary frequency of various fluids (i.e., ethanol, bromobenzene, and pure water) and of the Mie metamaterial comprising silicon spherical particles (radius $R_p = 100$ nm and filling factor $f = 0.5$) are shown in Fig. 2(a), while the permeability of the fluids and the Mie metamaterial vs imaginary frequency is plotted in the Fig. 2(a) inset. The requirement $\varepsilon_{Mie}(i\xi) < \varepsilon_{fluid}(i\xi)$ is alternately satisfied or violated over different frequency ranges, exhibiting one crossing in the Mie metamaterial curve with that of bromobenzene and two crossings with that of ethanol and pure water. As pointed out in Ref. [9], the type-I crossing that converts $\varepsilon_{Mie}(i\xi) > \varepsilon_{fluid}(i\xi)$ to $\varepsilon_{Mie}(i\xi) < \varepsilon_{fluid}(i\xi)$ from lower to higher frequencies accounts for the transition from repulsion to attraction of the Casimir force as the distance between two objects increased. This is because the lower-frequency range dominates the contribution to the Casimir force at larger separation distances, while the higher-frequency range dominates at smaller distances. The transition from attraction to repulsion as distance increased arises from the type-II crossing, which converts $\varepsilon_{Mie}(i\xi) < \varepsilon_{fluid}(i\xi)$ to $\varepsilon_{Mie}(i\xi) > \varepsilon_{fluid}(i\xi)$ from lower to higher frequencies. The repulsive-attractive transition is regarded as a stable equilibrium because two slabs will be pushed together by the attractive force when separating and be pulled apart by the repulsive force when approaching. The transition from attraction to repulsion, however, is unstable. When considering the other method whereby repulsion can be achieved, gold is regarded as the electric object and the Mie metamaterial as the magnetic object. In this method, the repulsive Casimir force is strengthened and stable equilibrium occurs at larger separations with increasing permeability of the Mie metamaterial.

Figure 2(b) shows the Casimir force between two semi-infinite plates composed of gold and the Mie metamaterial separated by the fluids of ethanol, bromobenzene, and pure water. The plot in Fig. 2(b) is normalized by the Casimir force between two perfectly electric conductors in vacuum, which is purely attractive. Therefore, the positive (negative) value of F/F_{PEC} corresponds to attraction (repulsion). An interesting behavior observed in Fig. 2(b) is that two, one, and zero transitions take place in ethanol, bromobenzene, and pure water, respectively, which correspond to the two, one, and two crossings in Fig. 2(a). A stable equilibrium at the separation $d \approx 132$ nm and an unstable equilibrium at the separation $d \approx 1.24\,\mu$m are found in ethanol, as a consequence of the one type-I and one type-II crossings of the $\varepsilon_{Mie}(i\xi)$ and $\varepsilon_{ethanol}(i\xi)$ curves. The repulsive-attractive transition at the separation $d \approx 127$ nm in bromobenzene arises from the contribution of the type-I crossing of the $\varepsilon_{Mie}(i\xi)$ and $\varepsilon_{bromobenzene}(i\xi)$ curves. The Casimir force in water is purely repulsive owing to the fact that the violation of $\varepsilon_{Mie}(i\xi) < \varepsilon_{fluid}(i\xi) < \varepsilon_{gold}(i\xi)$ occurs over an insufficiently wide range of frequencies and is

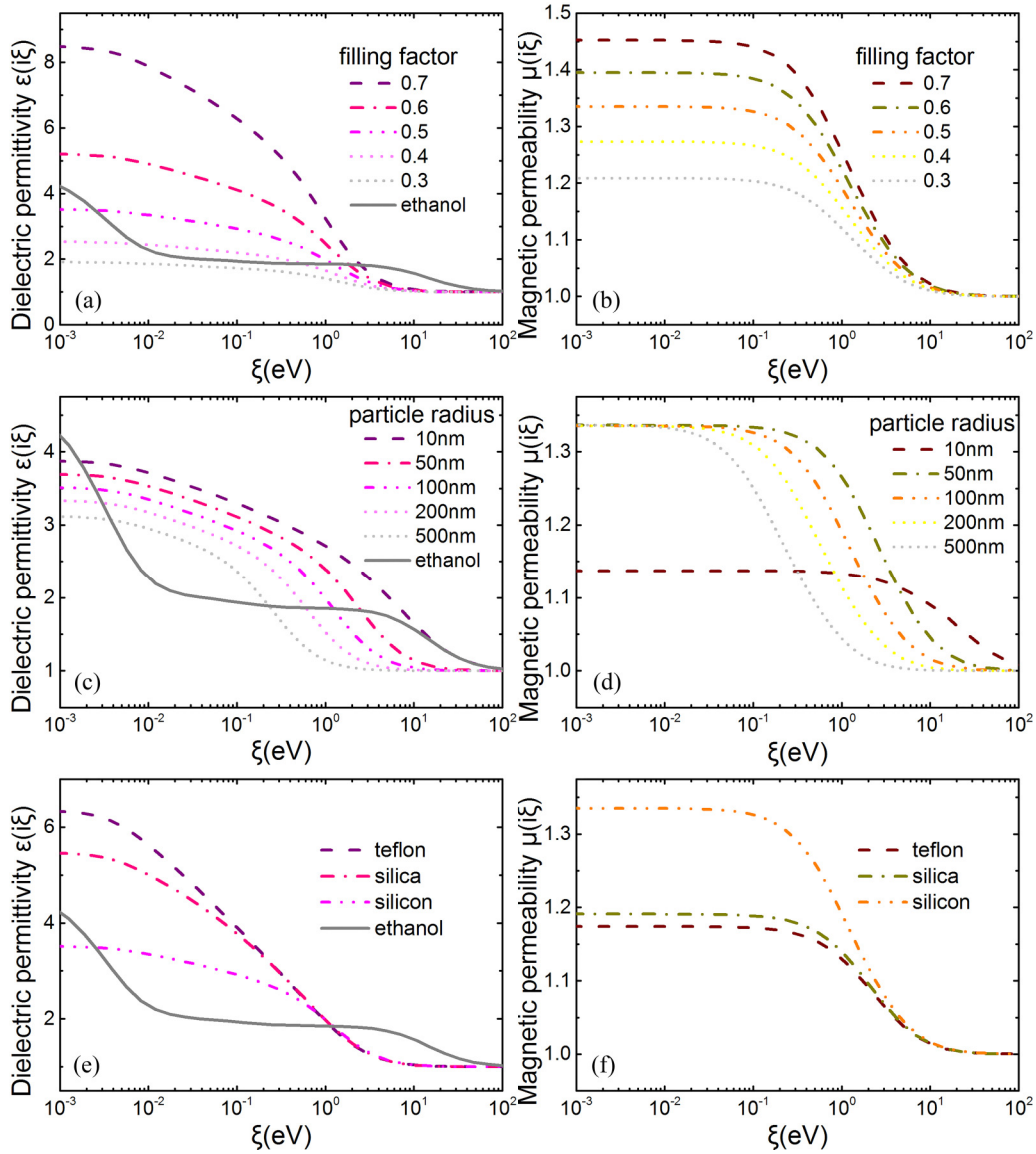

FIG. 3. (a) Permittivity and (b) permeability of Mie metamaterials with varying filling factor f of silicon particles (radius $R_p = 100\,\text{nm}$). (c) Permittivity and (d) permeability of Mie metamaterials with varying particle radius R_p of silicon particles ($f = 0.5$). (e) Permittivity and (f) permeability of Mie metamaterial for varying particle material ($R_p = 100\,\text{nm}$, $f = 0.5$).

therefore overwhelmed by the satisfaction of the requirement for achieving repulsion. Thus, a rough rule to predict the transition that uses the curve crossings of electromagnetic parameters alone may lead to incorrect results, though it can still provide guidance. In the following, only stable equilibrium is discussed, which is more desirable for potential applications.

To investigate the relationship between the separation distance of stable equilibrium and the constructive parameters of the Mie metamaterial, we first studied the effect of the constructive parameters' variations on the permittivity and permeability of the Mie metamaterial. The permittivity and permeability for various filling factors f, various particle radii R_p, and various particle materials are numerically calculated and illustrated in Fig. 3. The permittivity increases with increasing filling factor in Fig. 3(a), and a similar increase in permeability with filling factor increase is observed in Fig. 3(b). The increase of the permittivity occurs much more rapidly than that of the permeability, thus contributing to more Casimir attraction. When regarding the permittivity of ethanol, the repulsive-attractive transition is expected to take place in the filling factor range 0.4–0.6. Conversely, for the various particle radii, permittivity decreases as the particle size increases in Fig. 3(c). The effect of particle size on the permeability is much more complicated, as shown in Fig. 3(d). As the particle size increases, the permeability is strengthened in the lower frequencies but weakened in the higher frequencies. A feature worth noting is that both permittivity and permeability vary more dramatically with the filling-factor variation than with the particle size, leading to a greater deviation of equilibrium position with filling-factor modification than with particle size. Figures 3(e) and 3(f), respectively, plot the numerical calculations of the permittivity and permeability of a Mie metamaterial composed of three different dielectric particles: Teflon, silica, and silicon spheres.

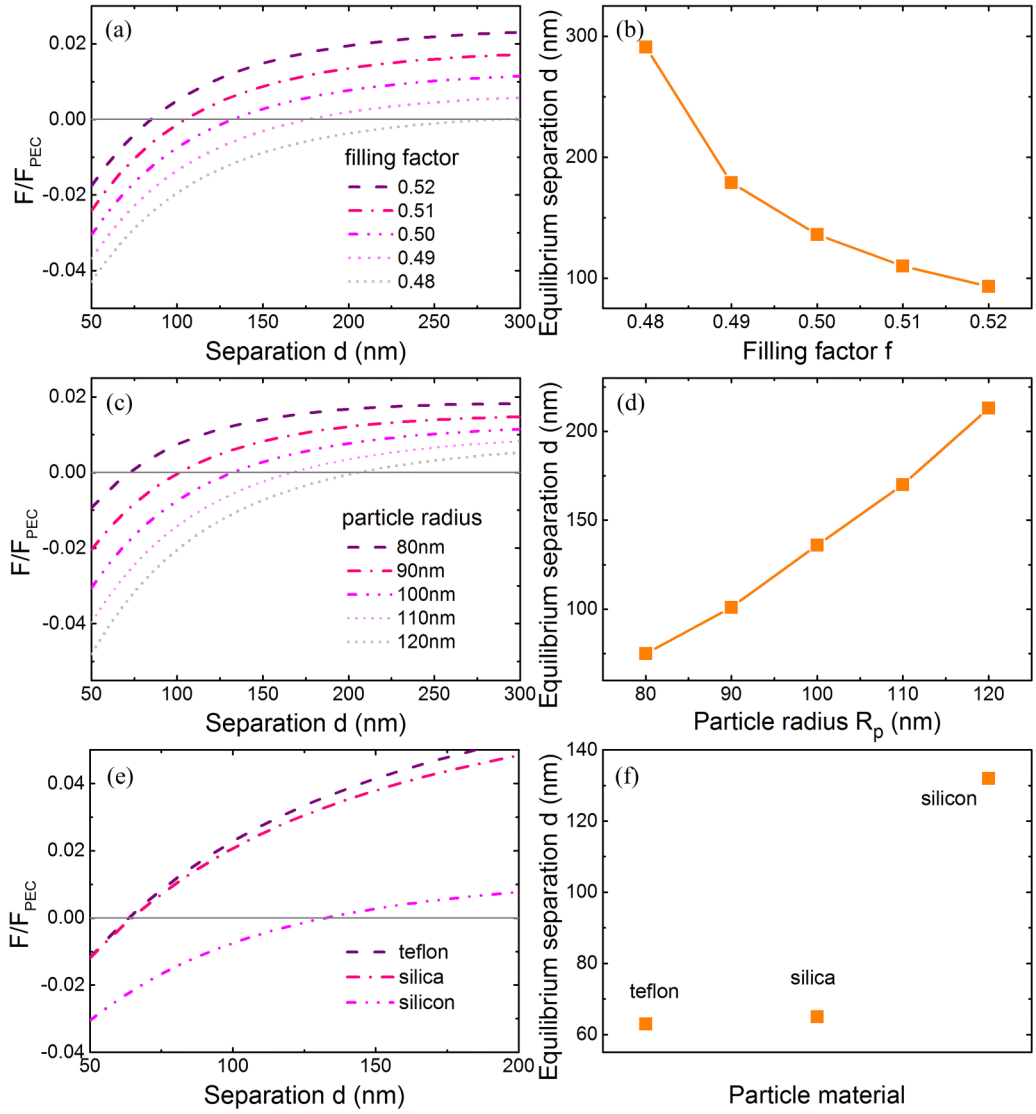

FIG. 4. Casimir force (F) between semi-infinite plates of gold and Mie metamaterial immersed in ethanol as a function of (a) filling factor f (silicon particles, $R_p = 100$ nm), (c) particle radius R_p (silicon particles, $f = 0.5$), and (e) particle material ($R_p = 100$ nm and $f = 0.5$). The F value is normalized by the Casimir force between perfect electric conductors in vacuum (F_{PEC}). (b), (d), and (f) are corresponding equilibrium separation distances obtained from (a), (c), and (e), respectively.

The permittivity is maximum and permeability is minimum for the Teflon particles, and vice versa for silicon particles. Therefore, silicon is expected to be a better candidate for achieving the repulsive-attractive transition.

The relative Casimir force F/F_{PEC} between the ethanol-separated gold slab and Mie metamaterial slab for varying filling factor f, varying particle radius R_p, and varying particle material is numerically calculated and plotted in Fig. 4, where F_{PEC} is the force between two perfectly electric conductors in vacuum. As mentioned above, a stable equilibrium may arise from a type-I crossing. This rough rule can be extended to specify that a type-I crossing at lower frequencies signifies a stable equilibrium at a greater separation distance. This extension of the rule is possible because more repulsion is contributed by the permittivity at high frequencies as the requirement $\varepsilon_{Mie}(i\xi) < \varepsilon_{fluid}(i\xi) < \varepsilon_{gold}(i\xi)$ is met as the $\varepsilon_{Mie}(i\xi)/\varepsilon_{fluid}(i\xi)$ curve crossing shifts to lower frequency. As expected, the transition from repulsion to attraction occurs when $f \approx 0.5$, as shown in Fig. 4(a). The equilibrium position deviates to greater separation distances with decreasing filling factor, corresponding to the type-I crossing of the $\varepsilon_{Mie}(i\xi)$ and $\varepsilon_{ethanol}(i\xi)$ curves to lower frequency with small filling factor. A similar change of equilibrium position to greater separation distances takes place in Fig. 4(b) as the particle size increases, which is mainly caused by the shift of the type-I crossing to lower frequency with increasing particle size. In particular, the deviation of stable equilibrium position is highly sensitive to a change of the filling factor, which should be considered carefully in Mie metamaterial applications in micro/nanoelectromagnetic devices. Another interesting phenomenon observed in Figs. 4(c) and 4(f) is that although the crossings of the $\varepsilon(i\xi)$ curves of ethanol with those of silicon, Teflon, and silica particles occur in close proximity, the equilibrium position of the silicon particles differs from that of

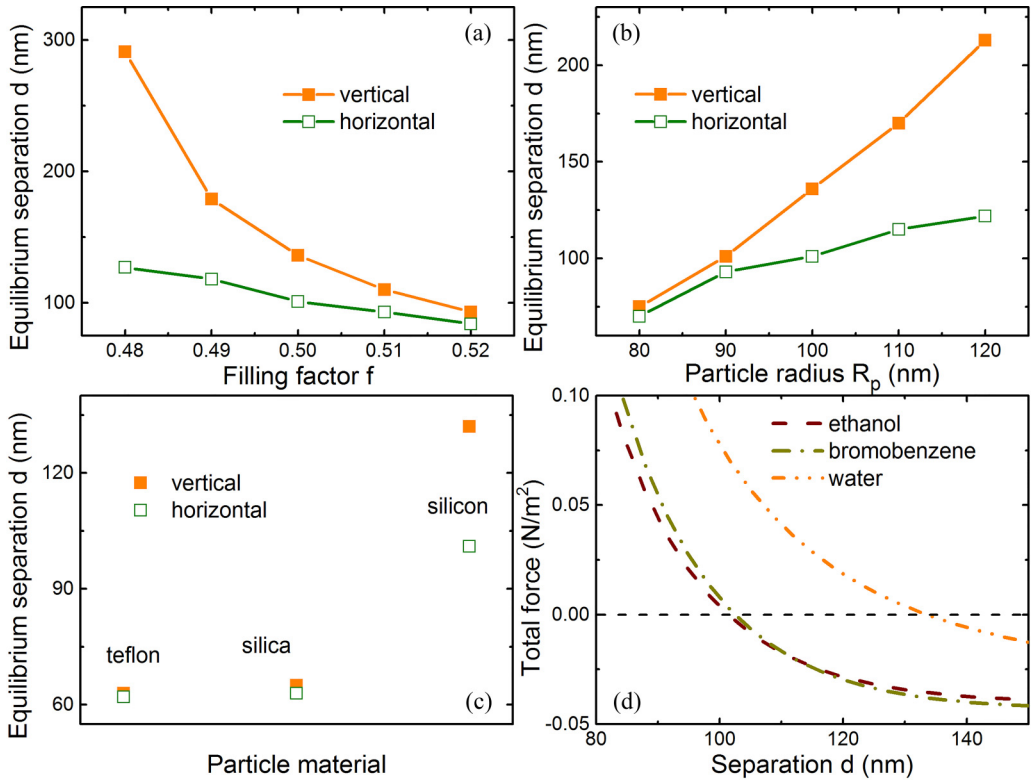

FIG. 5. Equilibrium separation distance of semi-infinite plates of gold and a Mie metamaterial immersed in ethanol for a system in a vertical (filled squares) and horizontal (empty squares) arrangement for varying (a) filling factor f, (b) particle radius R_p, and (c) particle material. All other parameters are the same as in Fig. 4. (d) Total force of semi-infinite plates of gold and a Mie metamaterial immersed in various fluids for a system in a horizontal arrangement. All other parameters are the same as in Fig. 2(a).

the Teflon and silica particles. This difference of equilibrium position is mainly owing to the great difference between the permittivity of the silicon particles and those of Teflon and silica particles in the lower-frequency range. Because an accurate result is obtained over the entire range of frequencies, the rule to predict the transition position using the permittivity curve crossing position alone fails in some situations, though it is still helpful. We obtain a wider range of equilibrium separation distances of 50–300 nm for all the parameters evaluated here, compared to the range of 50–200 nm obtained by natural materials [9]; and an equilibrium separation of a few micrometers can be reached with a larger filling factor. For experimental observations, a larger separation is more convenient. The particle size can be reduced to obtain a larger ratio of d/R_p. Furthermore, a specific separation distance can be obtained by selecting appropriate constructive parameters of the Mie metamaterial. A rough conclusion can be drawn here, where the stable equilibrium position can be tuned to greater separation distances by decreasing the filling factor, by increasing the particle size, and by selecting silicon instead of Teflon or silica. For all parameters investigated, the equilibrium position is the most sensitive to the filling factor.

We now consider the stable levitation in the system wherein a thin gold film is suspended over a Mie metamaterial substrate immersed in a fluid, where the stability is achieved by the balance of gravitational, buoyant, and Casimir forces. The gravitational and buoyant forces scale with the thickness of the gold film, as the surface area of gold film is fixed. The densities of gold (ρ_{gold}), ethanol (ρ_{ethanol}), and bromobenzene ($\rho_{\text{bromobenzene}}$) take the values 19.26, 0.789, and 1.5 g/cm^3, respectively. The separation distances of stable equilibrium of the gold film (thickness of 200 nm) suspended over a Mie metamaterial substrate (i.e., horizontal arrangement) separated by ethanol as a function of filling factor f, particle radius R_p, and particle material are numerically calculated and respectively plotted in Figs. 5(a)–5(c), and are compared to the system in a vertical arrangement. The law of the variation of equilibrium separation distance of the system in the horizontal arrangement as a function of these parameters is the same as that in the vertical arrangement, but all of the equilibrium separations of the system in the horizontal arrangement move to smaller values compared to the system in the vertical arrangement. This is because the repulsive Casimir force decays rapidly with increasing distance, whereupon the gravitational force becomes dominant and changes the effective force from repulsive to attractive at smaller separation distances. A feature worth noting is that the equilibrium separation distance is less sensitive to all investigated parameters in the horizontal arrangement than in the vertical arrangement, which can be used to modify the equilibrium separation distance more precisely. The total force of a gold film suspended over a Mie metamaterial substrate immersed in various fluids is plotted in Fig. 5(d), in which the positive (negative) value of the total force corresponds to repulsion (attraction). In the horizontal arrangement, a repulsive-attractive transition take place in the water-separated system at a separation distance $d \approx 135$ nm,

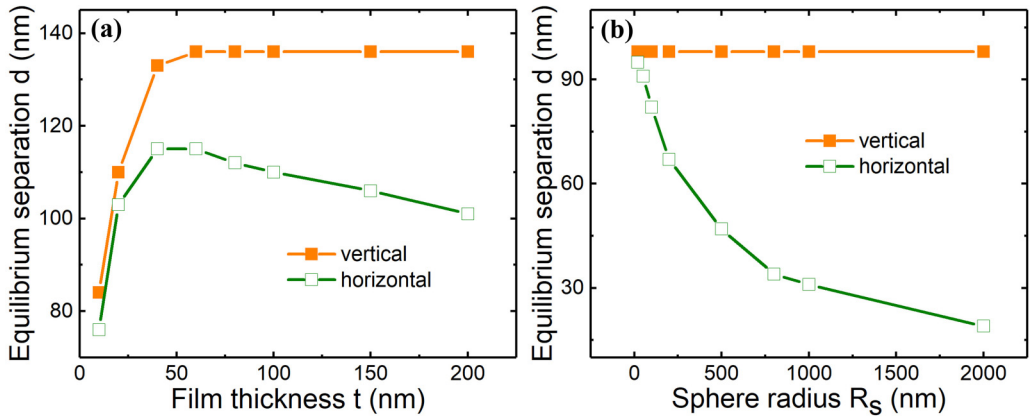

FIG. 6. Equilibrium separation distance of gold and Mie metamaterial immersed in ethanol for the (a) parallel-plate system in a vertical (solid squares) and horizontal (empty squares) arrangement for varying film thickness t, and the (b) sphere-plate system in a vertical (solid squares) and horizontal (empty squares) arrangement for varying sphere radius R_s (the leftmost points might be invalid). All other parameters are the same as in Fig. 2(a).

while the force is purely repulsive and no transition occurs in the vertical arrangement. This difference is also the result of gravity.

The effect of varying the Mie metamaterial constructive parameters on the equilibrium position is similar in the sphere-plate system in a vertical arrangement and that in a horizontal arrangement. Finally, we examine the effect of the geometric parameters of the parallel-plate and sphere–plate systems on the equilibrium position, including film thickness and sphere radius. For the parallel-plate system, the change of equilibrium position as a function of gold film thickness in the systems of vertical and horizontal arrangement is shown in Fig. 6(a). In the vertical arrangement, equilibrium is reached at greater separation distances as the gold film thickness increases and is asymptotic to the equilibrium values of the semi-infinite gold plate at large thicknesses. This difference in the equilibrium distance curves with film thickness is owing to the fact that the repulsive Casimir force is weakened with decreasing gold film thickness. In the horizontal arrangement, the equilibrium separation increases to a peak and then go down as film thickness increases. The upward trend of the separation distance with film thickness at smaller thicknesses is contributed to by the repulsive Casimir force, and that of the downward trend at larger thicknesses by the gravitational force. For the sphere-plate system in a vertical arrangement, the unique phenomenon wherein all transitions occur at the same separation distance for all sphere radii is observed, as shown in Fig. 6(b). This phenomenon arises from the fact that the Casimir force increases or decreases in proportion to the change of the sphere radius and the equilibrium position is invariant in the PFA method. It seems possible to assemble nanoparticles in a regular sequence by the same equilibrium position, however, the PFA method fails in the leftmost points in Fig. 6(b) when the curvature of the sphere is close to the separation distance [35,36]. In the system of a gold sphere levitated by a Mie metamaterial substrate, the separation distance of the stable suspension decreases as the sphere radius increases because the gravitational force increases more rapidly than the repulsive Casimir force with increasing sphere radius.

IV. CONCLUSIONS

We performed a theoretical analysis of the equilibrium phenomenon occurring between liquid-separated gold and Mie metamaterial for various geometries. A wider range of equilibrium separation is obtained with a Mie metamaterial than with natural materials. A stable levitation of a gold film and gold sphere over the Mie metamaterial substrates immersed in different fluids is also obtained. Roughly, the levitation position can be tuned to achieve a larger separation by decreasing the filling factor or increasing the particle size of the Mie metamaterial. Among the parameters, the equilibrium position is the most sensitive to the filling factor. The effect of the geometric parameters of the system in a vertical arrangement and in a horizontal arrangement is compared. The gravity force becomes the dominant force with increasing body size, but the interplay between the gravity and the Casimir force of tiny bodies is complicated. Our results serve as a guide for applications of Mie metamaterials in frictionless suspension in micro/nanofabrication technologies.

ACKNOWLEDGMENTS

This work is supported by the National Natural Science Foundation of China (Grants No. 51575297 and No. 51635009), the Science and Technology Plan of Shenzhen City (Grants No. JCYJ20160301154309393 and No. JCYJ20170817162252290), and the Chinese State Key Laboratory of Tribology.

[1] H. B. G. Casimir, Proc. K. Ned. Akad. Wet. **51**, 793 (1948).
[2] E. M. Lifshitz, Sov. Phys. JETP **2**, 73 (1956).
[3] I. E. Dzyaloshinskii, E. M. Lifshitz, and L. P. Pitaevskii, Adv. Phys. **10**, 165 (1961).

[4] J. N. Munday, F. Capasso, and V. A. Parsegian, Nature (London) **457**, 170 (2009).
[5] J. N. Munday and F. Capasso, Phys. Rev. A **75**, 060102 (2007).
[6] X. Liu and Z. M. Zhang, Phys. Rev. Appl. **5**, 034004 (2016).
[7] P. J. V. Zwol and G. Palasantzas, Phys. Rev. A **81**, 062502 (2010).
[8] V. Esteso, S. C. Palacios, and H. Míguez, J. Appl. Phys. **119**, 144301 (2016).
[9] A. W. Rodriguez, A. P. McCauley, D. Woolf, F. Capasso, J. D. Joannopoulos, and S. G. Johnson, Phys. Rev. Lett. **104**, 160402 (2010).
[10] T. H. Boyer, Phys. Rev. A **9**, 2078 (1974).
[11] R. Zhao, T. H. Koschny, E. N. Economou, and C. M. Soukoulis, Phys. Rev. D **82**, 065025 (2010).
[12] R. Zhao, J. Zhou, T. H. Koschny, E. N. Economou, and C. M. Soukoulis, Phys. Rev. Lett. **103**, 103602 (2009).
[13] A. P. McCauley R. K. Zhao, M. T. H. Reid, A. W. Rodriguez, J. F. Zhou, F. S. S. Rosa, J. D. Joannopoulos, D. A. R. Dalvit, C. M. Soukoulis, and S. G. Johnson, Phys. Rev. B **82**, 165108 (2010).
[14] G. Song, J. Xu, C. Zhu, P. He, Y. Yang, and S. Y. Zhu, Phys. Rev. A **95**, 023814 (2017).
[15] F. S. S. Rosa, D. A. R. Dalvit, and P. W. Milonni, Phys. Rev. Lett. **100**, 183602 (2008).
[16] R. Zeng, Y. P. Yang, and S. Y. Zhu, Phys. Rev. A **87**, 063823 (2013).
[17] J. Ma, Q. Zhao, and Y. Meng, Phys. Rev. B **89**, 075421 (2014).
[18] A. W. Rodriguez, J. D. Joannopoulos, and S. G. Johnson, Phys. Rev. A **77**, 062107 (2008).
[19] M. Levin, A. P. McCauley, A. W. Rodriguez, M. T. H. Reid, and S. G. Johnson, Phys. Rev. Lett. **105**, 090403 (2010).
[20] U. Leonhardt and T. G. Philbin, New J. Phys. **9**, 254 (2007).
[21] J. H. Wilson, A. A. Allocca, and V. Galitski, Phys. Rev. B **91**, 235115 (2015).
[22] P. Rodriguez-Lopez and A. G. Grushin, Phys. Rev. Lett. **112**, 056804 (2014).
[23] F. Capasso, J. N. Munday, D. Iannuzzi, and H. B Chan, IEEE J. Sel. Topics Quantum Electron. **13**, 400 (2007).
[24] S. de Man, K. Heeck, R. J. Wijngaarden, and D. Iannuzzi, Phys. Rev. Lett. **103**, 040402 (2009).
[25] Q. Zhao, J. Zhou, F. L. Zhang, and D. Lippens, Mater. Today **12**, 60 (2009).
[26] Q. Zhao, L. Kang, B. Du, H. Zhao, Q. Xie, X. Huang, B. Li, J. Zhou, and L. Li, Phys. Rev. Lett. **101**, 027402 (2008).
[27] R. G. Peng, Z. Q. Xiao, Q. Zhao, F. L. Zhang, Y. G. Meng, B. Li, J. Zhou, Y. C. Fan, P. Zhang, N. H. Shen, T. Koschny, and C. M. Soukoulis, Phys. Rev. X **7**, 011033 (2017).
[28] Q. Zhao, Z. Q. Xiao, F. L. Zhang, J. M. Ma, M. Qiao, Y. G. Meng, C. W. Lan, B. Li, J. Zhou, P. Zhang, N. H. Shen, T. Koschny, and C. M. Soukoulis, Adv. Mater. **27**, 6187 (2015).
[29] V. Yannopapas and A. Moroz, J. Phys.: Condens. Matter. **17**, 3717 (2005).
[30] S. J. Rahi, T. Emig, N. Graham, R. L. Jaffe, and M. Kardar, Phys. Rev. D **80**, 085021 (2009).
[31] B. V. Deriagin, I. I. Abrikosova, and E. M. Lifshitz, Q. Rev. Chem. Soc. **10**, 295 (1956).
[32] T. Emig, N. Graham, R. L. Jaffe, and M. Kardar, Phys. Rev. Lett. **99**, 170403 (2007).
[33] M. S. Tomas, Phys. Rev. A **66**, 052103 (2002).
[34] Z. Lenac, Phys. Rev. A **82**, 022117 (2010).
[35] H. B. Chan, Y. Bao, J. Zou, R. A. Cirelli, F. Klemens, W. M. Mansfield, and C. S. Pai, Phys. Rev. Lett. **101**, 030401 (2008).
[36] L. C. Lapas, A. P. Madrid, and J. M. Rubí, Phys. Rev. Lett. **116**, 110601 (2016).